## Original Article

# Applicability of Various EOS in Modeling the Pressure Dependence of the Volume Thermal Expansion Coefficient of Nanomaterials

Rajendra K. Mishra<sup>1</sup>, Om Prakash Gupta<sup>2</sup>

<sup>1,2</sup>Department of Physics, D.B.S. College, Govind Nagar, CSJM University Kanpur, Uttar Pradesh, India.

<sup>1</sup>Corresponding Author: rkmishra 625 @gmail.com

Received: 11 September 2025 Revised: 18 October 2025 Accepted: 04 November 2025 Published: 17 November 2025

Abstract - There is a great deal of scientific and technological interest in the mechanical and thermal behavior of nanomaterials under high-pressure compression situations. The volume thermal expansion coefficient, which is sensitive to changes in both temperature and pressure, is one of the main factors controlling this behavior. This study investigates the modeling of the pressure dependence of the volume thermal expansion coefficient in nanomaterials using several Equations of State (EOS), including the Murnaghan, Tait, Suzuki, and Shanker equations. The study evaluates each EOS's capacity to capture nanoscale phenomena such as surface tension and quantum confinement by comparing theoretical, experimental, and simulation data. According to the results, Suzuki EOS works best at lower pressures, whereas Murnaghan functions better at higher pressures. The study emphasizes the importance of selecting the appropriate EOS based on the material type and pressure range. It also indicates that modified or hybrid models are required for precise thermophysical predictions in applications including nanotechnology.

Keywords - Equation of State (EOS), Empirical, High Pressure Behavior, Material modeling, Volume Thermal Expansion Coefficient (VTEC).

#### 1. Introduction

The current focus of physics, chemistry, and engineering research is the study of nanocrystalline materials with dimensions less than 100 nm[1]. Applying high pressure is an effective method for altering the structure and characteristics of materials. Investigating materials under high pressure to understand the thermoelastic properties of solids has numerous applications in fields such as highpressure physics, materials science, geoscience, planetary studies, and astrophysics [2,3].

Researchers' comprehension of the stability of materials at the nanometer scale can be enhanced by research on compressibility and pressure-induced phase transitions for nanocrystalline materials. Due to the discovery of the fascinating features of these materials under harsh conditions, prior high-pressure studies of nanoparticles have attracted considerable interest [4,5]. Prior studies have indicated that size effects greatly influence the atomic structures and phase behavior of materials subjected to extreme pressure.

Recent researchers have investigated how the optical properties of nanoparticles vary with their size, which is relevant for Diverse applications such as optoelectronics, some memory devices, and energy storage. Semiconducting nanoparticles have garnered the interest of both researchers and engineers. Controllably synthesizing Ge nanoparticles requires reliable and straightforward synthetic techniques to advance these applications and gain a deeper understanding of their size-dependent characteristics [6].

Due to its simplicity in structure and geophysical significance, MgO with the NaCl-type cubic structure has been thoroughly investigated under high pressure. Due to its durability at high pressures, it can serve as a pressure calibration standard in experiments involving high temperatures and pressures. [7]

In clearly specified model systems comprising Cadmium Sulfide (CdSe) nanospheres or nanorods, the rock-salt structure was investigated concerning the composition, initial phase, and degree of ordering within their assemblies. It was discovered that these nanocrystal configurations exhibit ligand-tailorable reversibility during the solid-phase transition from rock salt to zinc blende. Kinetic barriers in the phase change were engineered via particle sintering to create adjustable ambient-pressure metastable rock-salt formations[8].

There are numerous physical, chemical, and environmental ways to create Titanium Dioxide Nanoparticles (TiO2-NPs), which are widely employed in daily life. Recent developments in the synthesis of TiO2-NPs and their use in wastewater treatment for the environment[9].

Reports from researchers, Multi-walled carbon nanotube composite sheets loaded with nickel, that are lightweight, flexible, and non-corrosive, can absorb microwaves in the S band (2-4 GHz). Indicating that substantial electromagnetic benefits are provided by modest filler a

In this study, Researchers present a simple theoretical framework for examining the  $\frac{\alpha_P}{\alpha_0}$  Of nanomaterials under pressure. Varied EOS that have been used to compute the change of  $\frac{\alpha_P}{\alpha_0}$  With varied high-pressure compression. Furthermore, the results obtained with alternative methods have been compared to find the applicability of various EOS in modeling the impact of pressure on the thermal expansion volume coefficient of nanomaterials.

# 2. Materials and Methods

## 2.1. Murnaghan EOS

The M-EOS [12] is predicated on the notion that, at any temperature, the elastic bulk modulus coefficient B isothermally linearly depends on pressure, that is

$$B(P, T) = B_0 + B_0'P$$
 (1)

The following is M-EOS with integrating (1) at constant temperature and utilizing the bulk modulus definition:

$$\frac{V}{V_0} = \left(1 + \frac{B_0'}{B_0}P\right)^{-\frac{1}{B_0'}} \tag{2}$$

So the Bulk modulus ratio

$$\frac{B_P}{B_0} = \left(\frac{V}{V_0}\right)^{-B_0/2} \tag{3}$$

Using thermodynamic approximation [13,14], the product of  $\propto_P$  and the Coefficient of bulk modulus  $B_P$  is constant [15].

$$\alpha_P B_P = \alpha_0 B_0$$

$$\frac{\alpha_P}{\alpha_0} = \frac{B_0}{B_P} = \left(\frac{V}{V_0}\right)^{B_0'}$$
(4)

This is the Murnaghan equation of state, useful to predict the pressure dependence coefficient of volume thermal expansion of nanomaterials.

#### 2.2. Tait EOS

For illustrates, the Compression exhibits a nonlinear function of applied pressure across several distinct liquid and solid classes [16]. M. Kumari and N. Dass [17].

$$1 - \frac{V(P,T)}{V(0,T)} = D \ln(1 + \frac{P}{C})$$

$$or \frac{V}{V_0} = 1 - D \ln(1 + \frac{P}{C})$$

Where D and C are assumed to be the parameters to be fitted, they are pressure-independent. Fitted, however, the above expression has a flaw in that, at high enough pressures, it produces negative volumes.

The conventional Tait equation is given by

$$\frac{V(P,T)}{V(0,T)} = 1 - \frac{1}{B_0^{\prime} + 1} \ln\left(\frac{B_0^{\prime} + 1}{B_0}\right) P + 1$$

Usual Tait equation) is written as [18].

$$\frac{B_P}{B_0} = \frac{V}{V_0} exp\left\{ \left( B_0^{/} + 1 \right) (1 - \frac{V}{V_0}) \right\}$$
 (5)

Using a well-known thermodynamic approximation

This is the relationship of the pressure dependent on  $\propto_P$ .

#### 2.3. Suzuki EOS

Mie-Gruneisen EOS[19] serves as the foundation for Gruneisen's theory of thermal expansion.

$$PV + X (V) = \gamma E_{th}$$
 Where 
$$X(V) = (d\Phi/dV)$$

Following the application of the Second-degree Taylor polynomial in the equation above with regard to the second order and subsequent solution, we obtain

$$\frac{V}{V_0} = \frac{\left[1 + 2B - (1 - \left(\frac{4BE_{Th}}{Q}\right))^{1/2}\right]}{2B}$$

Where  $B = (B_0^{/}-1)/2$ ,  $E_{Th}$  is the thermal energy,

$$Q=B_0V_0/\gamma_0$$

Where  $\gamma_0$  is the Gruneisen parameter,  $B_0$  is the Coefficient of volumetric elasticity, and the first pressure derivative  $B_0^f$ .

using expression [20]

$$P_{th} = \frac{\gamma E_{Th}}{V_0}$$

Using these values,

$$\frac{v}{v_0} - 1 = \frac{1 - \left[1 - 2\left(\frac{(B_0' - 1)}{B_0}\right) P_{Th}\right]^{\frac{1}{2}}}{(B_0' - 1)}$$

 $P_{Th}$  is the heat pressure

According to Shanker et al. [21], the preceding equation can be if  $P \neq 0$ 

$$\frac{V}{V_0} = \frac{\left[-\left[2\left(\frac{(B_0'-1)}{B_0}\right)(P-P_{Th})+1\right]^{\frac{1}{2}}+1\right]}{(B_0'-1)}+1$$

Now, if  $(P_{Th}=0)$  get

$$\frac{V}{V_0} = \frac{1 - \left[1 + 2\left(\frac{(B_0' - 1)}{B_0}\right)P\right]^{\frac{1}{2}}}{(B_0' - 1)} + 1$$

So

So 
$$\frac{B_P}{B_0} = \left[ \frac{V}{V_0} \left( 1 + (B_0' - 1)(1 - \frac{V}{V_0}) \right) \right]$$
 Apply relation (7)

$$\propto_P B_P = \propto_0 B_0$$

$$\frac{\alpha_P}{\alpha_0} = \left[ \frac{V}{V_0} \left( 1 + (B_0^{/} - 1)(1 - \frac{V}{V_0}) \right) \right]^{-1} \tag{8}$$

This eq. Represent the dependency of  $\propto_P$  On pressure.

#### 2.4. Shanker EOS

Shanker et al.[22] has applied the thermal expansion theory of Gruneisen, developed by Huang and Born, in which higher-order terms were included. These authors presented a new analytical form, that is,

$$\frac{v}{v_0} - 1 = \frac{1 - \left[1 + 2\left(\frac{(B_0' + 1)}{B_0}\right) P_{Th}\right]^{\frac{1}{2}}}{(B_0' + 1)}$$

Kushwaha and Shanker argued that when pressure p≠0, then,

$$\frac{v}{v_0} - 1 = \frac{1 - \left[1 + 2\left(\frac{(B_0' + 1)}{B_0}\right)(P - P_{Th})\right]^{\frac{1}{2}}}{(B_0' + 1)}$$
When  $P_{th} = 0$  
$$\frac{v}{v_0} - 1 = \frac{1 - \left[1 + 2\left(\frac{(B_0' + 1)}{B_0}\right)P\right]^{\frac{1}{2}}}{(B_0' + 1)}$$

$$\frac{B_{P}}{B_{0}} = \left[ \frac{V}{V_{0}} \left( 1 + (B_{0}^{/} + 1)(1 - \frac{V}{V_{0}}) \right) \right]$$
(9)

Using relation

$$\propto_P B_P = \propto_0 B_0$$

$$\frac{\alpha_P}{\alpha_0} = \left[ \frac{V}{V_0} \left( 1 + (B_0' + 1)(1 - \frac{V}{V_0}) \right) \right]^{-1} \tag{10}$$

This eq. Represent the variation of  $\propto_P$  With pressure at constant temperature.

## 3. Results and Discussion

Table 1. Input data with references

Nanomaterials	B <sub>0</sub> (GPa)	$\boldsymbol{B_0^{/}}$
Ge(13nm)	112[23]	4[23]
MgO	179[24]	1.5[24]
CdSe(5.4nm)	37[25]	11[25]
TiO2(Rutile Phase)	211[26]	8[27]
Nickel-Encapsulated MWCNT	179.8[28]	5.3[28]
Iron-Encapsulated MWCNT	167[28]	8.5[28]

Table 2. Calculated values of  $\frac{\alpha_p}{\alpha_c}$  Of Germanium Nanomaterial Under High Compression.

Germanium nanomaterial (Ge(13nm))				
Volume Compression ratio ( $\frac{V}{V_0}$ )	Pressure-dependent Coefficient of Volume Thermal Expansion $\frac{\alpha_p}{\alpha_0}$			
V 0	Murnaghan	Tait	Suzuki	Shanker
1	1.00	1	1.00	1.00
0.95	0.81	0.82	0.92	0.84
0.9	0.66	0.67	0.85	0.74
0.85	0.52	0.56	0.81	0.67
0.8	0.41	0.46	0.78	0.63
0.77	0.35	0.41	0.77	0.60
0.7	0.24	0.32	0.75	0.57
0.65	0.18	0.27	0.75	0.56
0.6	0.13	0.23	0.76	0.56

Table 3. Calculated values of  $\frac{\alpha_p}{\alpha_0}$  of MgO nanomaterial  $\,$  under high compression

(MgO) Nanomaterial				
Volume Compression	Pressure-dependent Coefficient of Volume Thermal Expansion $\frac{\propto_p}{\propto_0}$			
ratio $(\frac{r}{V_0})$	Murnaghan	Tait	Suzuki	Shanker
1	1.00	1	1.00	1.00
0.95	0.93	0.93	1.03	0.94
0.9	0.85	0.87	1.06	0.89
0.85	0.78	0.81	1.09	0.86
0.8	0.72	0.76	1.14	0.83
0.77	0.68	0.73	1.16	0.82
0.7	0.59	0.67	1.24	0.82
0.65	0.52	0.64	1.31	0.82
0.6	0.46	0.61	1.39	0.83

Table 4. Calculated values of  $\frac{\alpha_p}{\alpha_0}$  of CdSe Nanomaterial Under High Compression.

	∝ <sub>0</sub>			
CdSe nanomaterials				
Volume Compression	Pressure-dependent Coefficient of Volume Thermal Expansion $\frac{\propto_p}{\propto_0}$			
ratio $(\frac{v}{V_0})$	Murnaghan	Tait	Suzuki	Shanker
1	1.00	1.00	1.00	1.00
0.95	0.57	0.58	0.70	0.66
0.9	0.31	0.33	0.56	0.51
0.85	0.17	0.19	0.47	0.42
0.8	0.09	0.11	0.42	0.37
0.77	0.06	0.08	0.39	0.35
0.7	0.02	0.04	0.36	0.31
0.65	0.01	0.02	0.34	0.30
0.6	0.00	0.01	0.33	0.29

Table 5. Calculated values of  $\frac{\alpha_p}{\alpha_0}$  Of TiO<sub>2</sub> Nanomaterial Under High Compression.

TiO <sub>2</sub> nanomaterials				
Volume ratio $(\frac{V}{V_0})$	Pressure-dependent Coefficient of Volume Thermal Expansion $\frac{\alpha_p}{\alpha_0}$			
	Murnaghan	Tait	Suzuki	Shanker
1	1.00	1.00	1.00	1.00
0.95	0.66	0.67	0.78	0.73
0.9	0.43	0.45	0.65	0.58
0.85	0.27	0.30	0.57	0.50
0.8	0.17	0.21	0.52	0.45
0.77	0.12	0.16	0.50	0.42
0.7	0.06	0.10	0.46	0.39
0.65	0.03	0.07	0.45	0.37
0.6	0.02	0.05	0.44	0.36

Table 6. Calculated values of  $\frac{\alpha_p}{\alpha_0}$  Of Ni-Filled MWCNT Nanomaterial Under High Compression.

Ni-Filled MWCNT				
Volume Compression ratio ( $\frac{V}{V_0}$ )	Pressure-dependent Coefficient of Volume Thermal Expansion $\frac{\alpha_P}{\alpha_0}$			
	Murnaghan	Tait	Suzuki	Shanker
1	1.00	1.00	1.00	1.00
0.95	0.76	0.77	0.87	0.80
0.9	0.57	0.59	0.78	0.68
0.85	0.42	0.46	0.72	0.60
0.8	0.31	0.35	0.67	0.55
0.77	0.25	0.30	0.65	0.53
0.7	0.15	0.22	0.62	0.49
0.65	0.10	0.17	0.61	0.48
0.6	0.07	0.13	0.61	0.47

Table 7. Calculated values of  $\frac{\alpha_p}{\alpha_0}$  Of Fe-Filled MWCNT Nanomaterial Under High Compression.

	Fe-Filled MWCNT					
Volume Compression	Pressure-dependent Coefficient of Volume Thermal Expansion $\frac{\frac{\alpha_P}{\alpha_0}}{\alpha_0}$					
ratio $(\frac{V}{V_0})$	Murnaghan Tait Suzuki Shanker					
1	1.00	1.00	1.00	1.00		
0.95	0.65	0.65	0.77	0.71		
0.9	0.41	0.43	0.63	0.57		
0.85	0.25	0.28	0.55	0.49		
0.8	0.15	0.19	0.50	0.43		
0.77	0.11	0.15	0.48	0.41		
0.7	0.05	0.08	0.44	0.37		
0.65	0.03	0.06	0.42	0.36		
0.6	0.01	0.04	0.42	0.35		

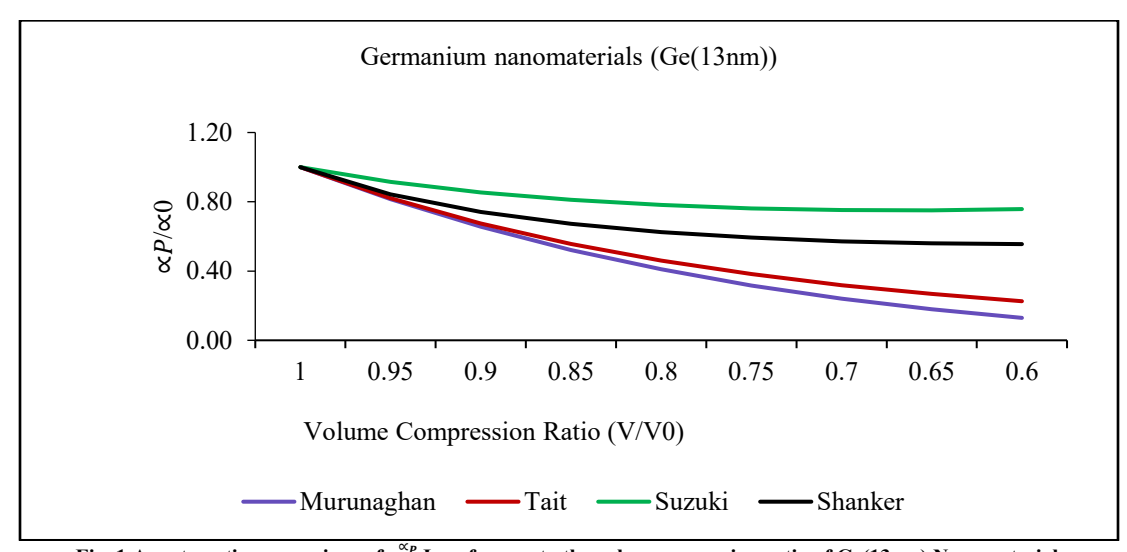


Fig. 1 A systematic comparison of  $\frac{\alpha_p}{\alpha_0}$  In reference to the volume expansion ratio of Ge(13nm) Nanomaterial.

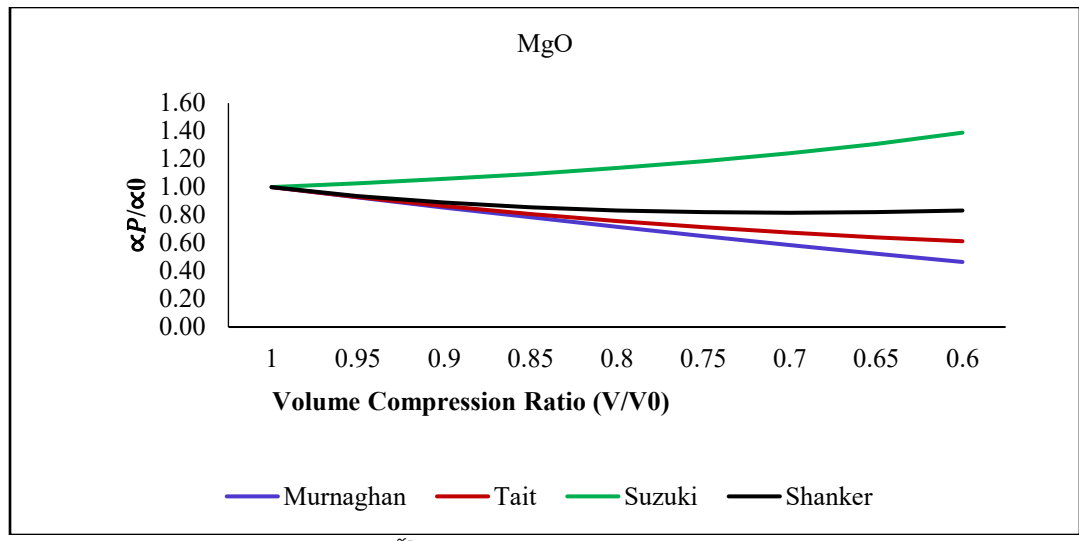


Fig. 2 A systematic comparison of  $\frac{\kappa_p}{\kappa_0}$  In reference to the volume expansion ratio of MgO Nanomaterial.

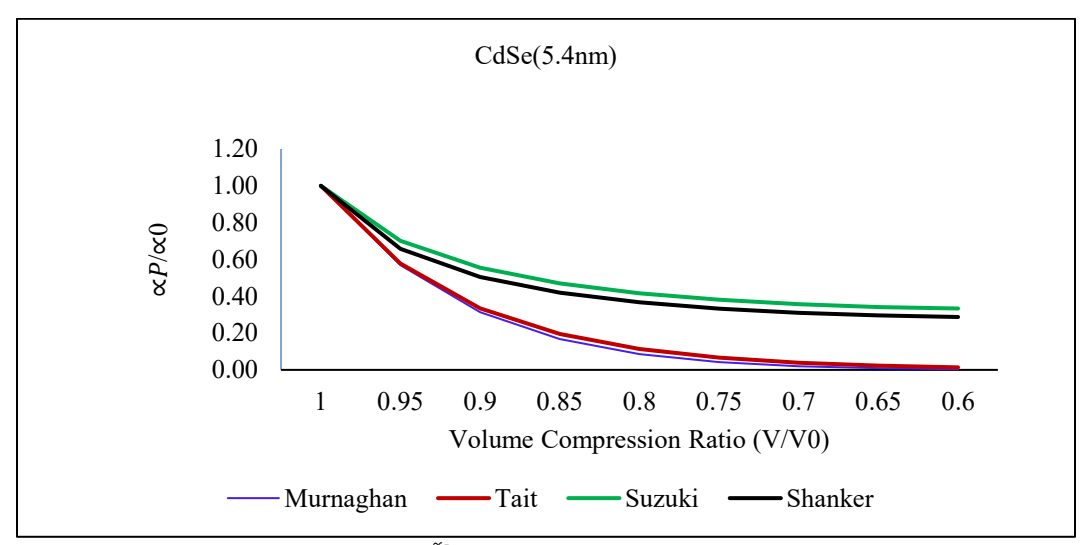


Fig. 3 A systematic comparison of  $\frac{\kappa_p}{\kappa_0}$  with respect to volume expansion ratio of CdSe Nanomaterial.

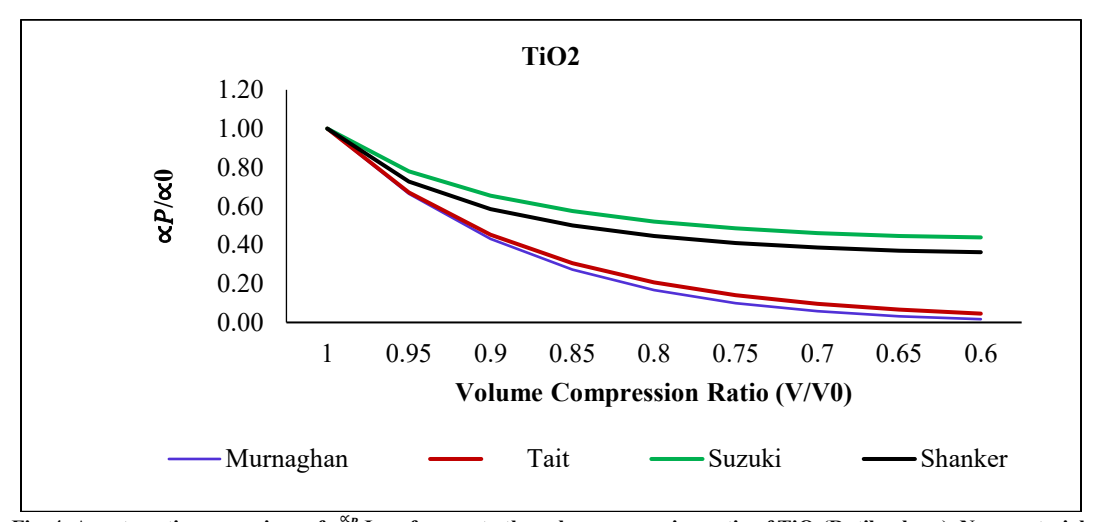


Fig. 4 A systematic comparison of  $\frac{\alpha_p}{\alpha_0}$  In reference to the volume expansion ratio of TiO<sub>2</sub>(Rutile phase) Nanomaterial.

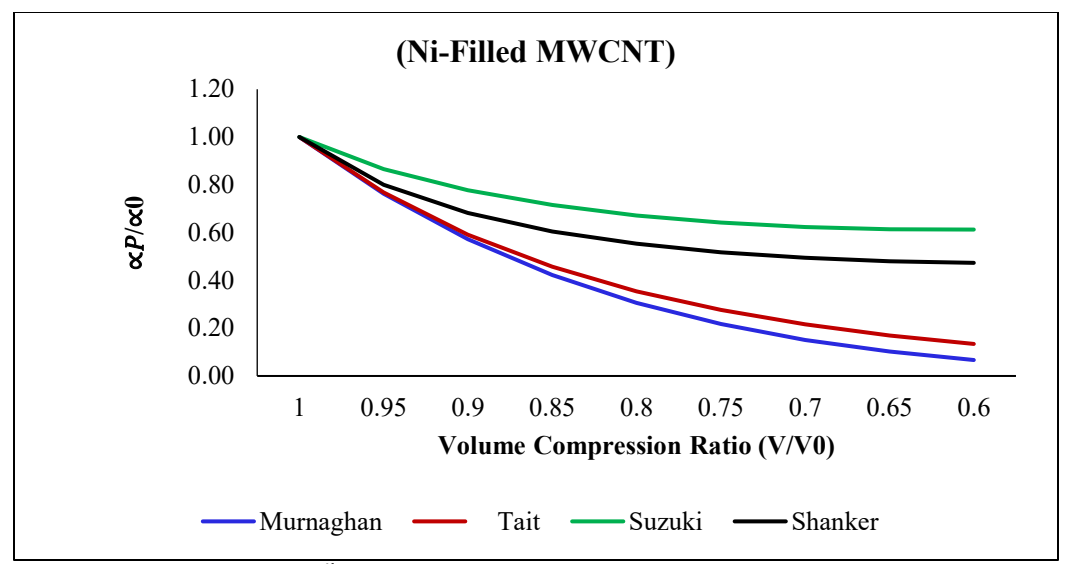


Fig. 5 A systematic comparison of  $\frac{\alpha_p}{\alpha_0}$  In reference to the volume expansion ratio of Ni-filled MWCNT Nanomaterial.

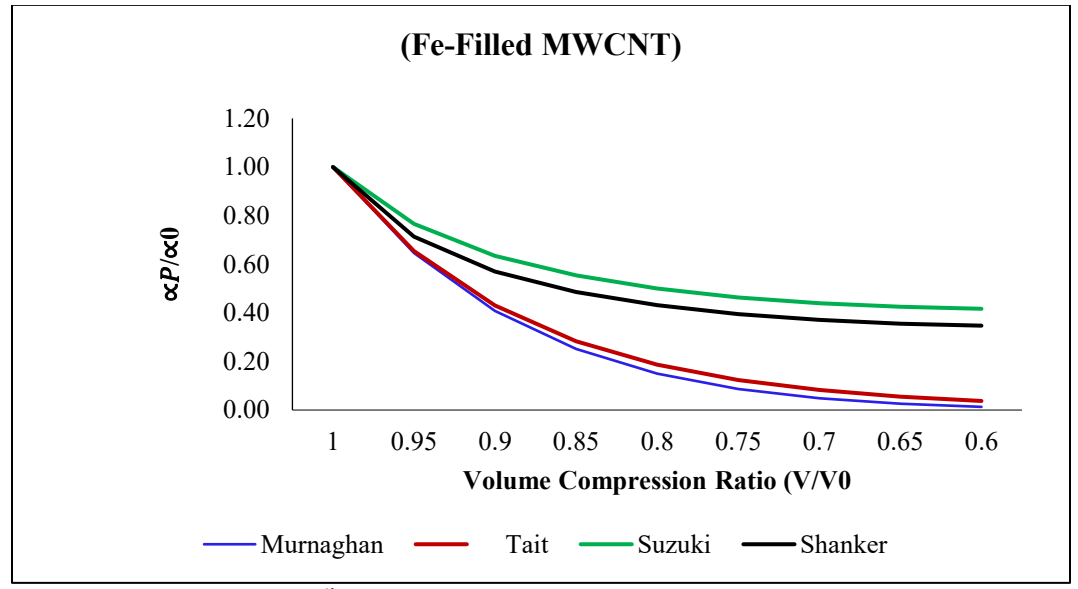


Fig. 6 A systematic comparison of  $\frac{\alpha_p}{\alpha_0}$  With respect to the volume expansion ratio of Fe-filled MWCNT Nanomaterial.

In the present work, the authors have described four different forms of pressure-dependent Coefficient of volume thermal expansion: Murnaghan, Tait, Suzuki, and Shanker. All contain only one parameter  $B_0$  at zero pressure. These values of  $B_0$  and  $B_0$  have been reported by [23-28]. The estimations of  $\frac{\alpha_P}{\alpha_0}$  Regarding nanomaterials, Germanium (13 nm), MgO, CdSe(5.4nm), TiO2(Rutile Phase), Ni-Filled MWCNT, and Fe-Filled MWCNT were calculated using equations (4), (6), (8), and (10) for specified increments of V/V0. The controlling parameter values,  $B_0$  and  $B_0$ , are derived from previous work and are displayed in Table 1. The dependency of  $\frac{\alpha_P}{\alpha_0}$  With compression displayed in

Figures 1 to 6. In all the Figures, It is found that the volume of the nanoparticle decreases as the increase in pressure increases and  $\frac{\alpha_P}{\alpha_0}$  Decreases with compression increases. At a low pressure value, all curves with the four EOSs are relatively close to each other. The result of all EOSs for  $\frac{\alpha_P}{\alpha_0}$  Significantly close up to relative compression of .95 for all nanoparticles. Increasing compression causes the curves of all EOSs to exhibit more divergence. The variation in  $\frac{\alpha_P}{\alpha_0}$  The relative volume of MgO greatly differs with the Suzuki EOS and Murnaghan EOS compared to other

nanomaterials. Thus, the variation tendency of  $\frac{\alpha_P}{\alpha_0}$  With fractional volume using four EOS, they are similar to all compression and reach the minimum value at compression V/Vo = .6 except MgO nanomaterials at this compression, MgO shows more deviation compared to other taken nanomaterials in this research.

## 4. Conclusion

Crucial details on the nanoscale thermodynamic behavior of materials can be gained by examining the suitability of different Equations of State (EOS) for simulating the pressure dependence of the volume thermal expansion coefficient.  $\frac{\alpha_P}{\alpha_0} \qquad \text{Of nanomaterials. Given their distinct surface-to-volume ratio, quantum confinement effects, and modified interatomic potentials, it is clear from a comparison of models like the Murnaghan, Tait, Suzuki, and Shanker semi-empirical EOS that no one EOS can be applied to all nanomaterials. The nature of the material, its bonding properties, and the pressure range taken into consideration all have a substantial impact on how well an EOS predicts <math display="block">\frac{\alpha_P}{\alpha_0}$  Under variable volume compression. The Suzuki EOS

performs well at lower compression but tends to depart from its optimal performance at higher compression. The Murnaghan EOS generally offers better agreement with experimental and simulation results at high compression among the models examined.

This study highlights the importance of selecting the appropriate EOS for a specific set of nanomaterials and operating conditions. The results also highlight how crucial it is to construct modified equations or include nanoscale-specific elements in conventional EOS in order to depict the behavior of nanomaterials under pressure more accurately. The design and optimization of nanomaterials for high-pressure applications, including energy storage, catalysis, and nanoelectronics, depend on these developments.

In conclusion, future research must concentrate on improving existing models or creating new ones that reflect the unique physics at the nanoscale, even though classical EOS offers a fundamental framework. This will guarantee more precise predictions of mechanical and thermal properties under various pressure circumstances. Therefore, the proposed formulation may be useful for future Highpressure analysis of nanomaterial compressibility.

#### References

- [1] H. Gleiter, "Nanostructured Materials: Basic Concepts and Microstructure," *Acta Mater*, vol. 48, no. 1, pp. 1–29, 2000. [CrossRef] [Google Scholar] [Publisher Link]
- [2] Manaf A. Mahammed, and Hamsa B. Mohammed, "Variation of Bulk Modulus, Its First Pressure Derivative, and Thermal Expansion Coefficient with Applied High Hydrostatic Pressure," *Advances in Condensed Matter Physics*, 2023, [CrossRef] [Google Scholar] [Publisher Link]
- [3] Ho Khac Hieu, and Nguyen Ngoc Ha, "High Pressure Melting Curves of Silver, Gold and Copper," *AIP Advances*, vol. 3, 2013. [CrossRef] [Google Scholar] [Publisher Link]
- [4] Juanying Li et al., "Size and Morphology Effects on the High Pressure Behaviors of Mn<sub>3</sub>O<sub>4</sub> Nanorods," *Nanoscale Advances*, vol. 2, pp. 5841–5847, 2020. [CrossRef] [Google Scholar] [Publisher Link]
- [5] Feng Bai et al., "Pressure Induced Nanoparticle Phase Behavior, Property, and Applications," *Chemical Reviews*, vol. 119, no. 12, pp. 7673–7717, 2019. [CrossRef] [Google Scholar] [Publisher Link]
- [6] Dimitri D. Vaughn, and Raymond E. Schaak, "Synthesis, Properties and Applications of Colloidal Germanium and Germanium-based Nanomaterials," *Chemical Society Reviews*, vol. 42, no. 7, pp. 2861–2879, 2013. [CrossRef] [Google Scholar] [Publisher Link]
- [7] Z.J. Liu et al., "High Pressure Melting of MgO," *Physics Letters A*, vol. 353, no. 2–3, pp. 221–225, 2006. [CrossRef] [Google Scholar] [Publisher Link]
- [8] Tianyuan Xiao et al., "Nanocrystals with Metastable High-pressure Phases Under Ambient Conditions," *Science*, vol. 377, no. 6608, pp. 870–874, 2022. [CrossRef] [Google Scholar] [Publisher Link]
- [9] Hemra Hamrayev, Serdar Korpayev, and Kamyar Shameli, "Advances in Synthesis Techniques and Environmental Applications of TiO2 Nanoparticles for Wastewater Treatment: A Review," *Journal of Research in Nanoscience and Nanotechnology*, vol. 12, no. 1, pp. 1–24, 2024. [CrossRef] [Google Scholar] [Publisher Link]
- [10] Rajesh Kumar Srivastava et al., "Ni Filled Flexible Multi-walled Carbon Nanotube-polystyrene Composite Films as Efficient Microwave Absorbers," *Applied Physics Letters*, vol. 99, no. 11, 2011. [CrossRef] [Google Scholar] [Publisher Link]
- [11] A. Jedrzejewska et al., "Synthesis and Characterization of Iron-filled Multi-walled Nanotubes," *Materials Science-Poland*, vol. 29, pp. 299–304, 2011. [CrossRef] [Google Scholar] [Publisher Link]
- [12] F.D. Murnaghan, "The Compressibility of Media Under Extreme Pressures," *Proceedings of the National Academy of Sciences*, vol. 30, no. 9, pp. 244-247, 1944. [CrossRef] [Google Scholar] [Publisher Link]
- [13] J. Shanker, and M. Kumar, "Thermodynamic Approximations in High-pressure and High-Temperature Physics of Solids," *Physica Status Solidi*, vol. 179, no. 2, pp. 351-356, 1993. [CrossRef] [Google Scholar] [Publisher Link]

- [14] Jeewan Chandra, and Kuldeep Kholiya, "Compression of Nanomaterials Under Pressure," *Journal of Taibah University for Science*, vol. 10, no. 3, pp. 386–392, 2016. [CrossRef] [Google Scholar] [Publisher Link]
- [15] Deepika P. Joshi, and Anjali Senger, "Applicability of Different Isothermal EOS at Nanomaterials," *Physics Research International*, 2013. [CrossRef] [Google Scholar] [Publisher Link]
- [16] H. Schlosser, and J. Ferrante, "An Accurate Analytic Approximation to the Non-Linear Change in Volume of Solids with Applied Pressure," *Journal of Physics: Condensed Matter*, vol. 1, no. 16, 1989. [CrossRef] [Google Scholar] [Publisher Link]
- [17] N. Dass, and M. Kumari, "Derivation of Some Equations of State for Solids. A New Approach," Basic Solid State Physics, vol. 127, no. 1, pp. 103-108, 1985. [CrossRef] [Google Scholar] [Publisher Link]
- [18] Orson L. Anderson, and Donald G. Isaak, "The Dependence of the Anderson-Grüneisen Parameter δT upon Compression at Extreme Conditions," *Journal of Physics and Chemistry of Solids*, vol. 54, no. 2, pp. 221–227, 1993. [CrossRef] [Google Scholar] [Publisher Link]
- [19] Mario P. Tosi, "Cohesion of Ionic Solids in the Born Model," *Solid State Physics*, vol. 16, pp. 1–120, 1964. [CrossRef] [Google Scholar] [Publisher Link]
- [20] Munish Kumar, "A Comparative Study of Suzuki and Kumar Formulations for Thermal Expansivity," *Indian Journal of Pure & Applied Physics*, vol. 42, 2004. [Google Scholar] [Publisher Link]
- [21] J. Shanker, S.S. Kushwaha, and P. Kumar, "Theory of Thermal Expansivity and Bulk Modulus for MgO and Other Minerals at High Temperatures," *Physica B: Condensed Matter*, vol. 233, no. 1, pp. 78-83, 1997. [CrossRef] [Google Scholar] [Publisher Link]
- [22] J. Shanker, B. Singh, and S.S. Kushwaha, "On the High-Pressure Equation of State for Solids," *Physica B: Condensed Matter*, vol. 229, no. 3-4, pp. 419-420, 1997. [CrossRef] [Google Scholar] [Publisher Link]
- [23] Pratyay Chattopadhyay, G.R. Patel, and T.C. Pandya, "Effect of Size and Shape on Thermo-Elastic Properties of Nano-Germanium," *International Journal of Nanoscience and Nanotechnology*, vol. 17, no. 3, pp. 141-145, 2021. [Google Scholar] [Publisher Link]
- [24] Rohit Gupta, and Mohit Gupta, "Bulk Modulus of Second-order Pressure Derivative for Nanomaterials," *Bulletin of Materials Sciences*, vol. 44, 2021. [CrossRef] [Google Scholar] [Publisher Link]
- [25] Sarah H. Tolbert, and A.P. Alivisatos, "The Wurtzite to Rock Salt Structural Transformation in CdSe Nanocrystals Under High Pressure," *The Journal of Chemical Physics*, vol. 102, pp. 4642–4656, 1995. [CrossRef] [Google Scholar] [Publisher Link]
- [26] Varghese Swamy et al., "Mechanical Properties of Bulk and Nanoscale TiO2 Phases," *Journal of Physics and Chemistry of Solids*, vol. 69, no. 9, pp. 2332–2335, 2008. [CrossRef] [Google Scholar] [Publisher Link]
- [27] Uma D. Sharma, and M. Kumar, "Effect of Pressure on Nanomaterials," *Physica B: Condensed Matter*, vol. 405, no. 13, pp. 2820–2826, 2010. [CrossRef] [Google Scholar] [Publisher Link]
- [28] H.K. Poswal et al., "High-pressure Behavior of Ni-filled and Fe-filled Multiwalled Carbon Nanotubes," *Physica Status Solidi (b)*, vol. 244, no. 10, pp. 3612–3619, 2007. [CrossRef] [Google Scholar] [Publisher Link]